



## Research articles

Co<sub>5/3</sub>Nb<sub>1/3</sub>BO<sub>4</sub>: A new cobalt oxyborate with a complex magnetic structure

N.V. Kazak<sup>a,\*</sup>, N.A. Belskaya<sup>b</sup>, E.M. Moshkina<sup>a</sup>, L.N. Bezmaternykh<sup>a</sup>, A.D. Vasiliev<sup>a,c</sup>,  
J. Bartolome<sup>d</sup>, A. Arauzo<sup>d,e</sup>, D.A. Velikanov<sup>a</sup>, S.Yu. Gavrilkin<sup>f</sup>, M.V. Gorev<sup>a,c</sup>, G.S. Patrino<sup>a,c</sup>,  
S.G. Ovchinnikov<sup>a,c</sup>

<sup>a</sup> Kirensky Institute of Physics, FRC SB RAS, Krasnoyarsk, Russia

<sup>b</sup> Reshetnev Siberian State University of Science and Technology, Krasnoyarsk, Russia

<sup>c</sup> Siberian Federal University, Krasnoyarsk, Russia

<sup>d</sup> Instituto de Nanociencia y Materiales de Aragón (INMA), CSIC-Universidad de Zaragoza and Departamento de Física de la Materia Condensada, 50009 Zaragoza, Spain

<sup>e</sup> Servicio de Medidas Físicas, Universidad de Zaragoza, Zaragoza, Spain

<sup>f</sup> P.N. Lebedev Physical Institute of RAS, 119991 Moscow, Russia



## ARTICLE INFO

Keywords:  
Warwickites  
Ferrimagnet

## ABSTRACT

Needle-shape single crystals of Co<sub>5/3</sub>Nb<sub>1/3</sub>BO<sub>4</sub> warwickite were grown using the flux technique. X-ray diffraction measurements have revealed an orthorhombic structure (Sp. Gr. *Pbnm*) where the octahedral M1 site is occupied by a mixture of Co<sup>2+</sup>/Nb<sup>5+</sup> ions and the M2 site is exclusively filled by Co<sup>2+</sup> ions. Using *dc* magnetization measurements it was established that the new material undergoes two magnetic transitions: an antiferromagnetic transition at  $T_{N1} = 27$  K and a ferrimagnetic one at  $T_{N2} = 14$  K, below which a hysteresis cycle opens. Both magnetic transitions are marked by anomalies in the specific heat. High magnetic anisotropy with *c*-axis as a hard magnetization direction was detected.

## 1. Introduction

The transition metal borates and oxyborates are important for applications, for example, for lithium-ion (LIBs) and sodium-ion (SIBs) batteries [1–5] and also for fundamental interest in the interplay between charge, orbital, spin, and lattice degrees of freedom. Iron borate, FeBO<sub>3</sub>, with calcite structure has been studied intensively since 1972 when a spontaneous magnetic moment at room temperature and simultaneous transparency in the visible spectral range has been reported [6,7]. At high pressure, this material undergoes a spin-state crossover accompanied by insulator-semiconductor electronic transition with a drastic drop of the optical absorption edge [8,9]. Later, the iron oxyborates with warwickite (Fe<sub>2</sub>BO<sub>4</sub>) [10] and ludwigite (Fe<sub>3</sub>BO<sub>5</sub>) [11] structures have attracted large attention due to charge-ordering (CO). The Fe<sub>2</sub>BO<sub>4</sub> shows an incommensurate charge order below  $T_{CO} = 340$  K, while dimer states were found in Fe<sub>3</sub>BO<sub>5</sub> below  $T_{CO} = 283$  K. In both materials, the charge ordering is accompanied by the structural and electronic transitions as it was found employing polarized resonant X-ray diffraction, Mössbauer spectroscopy, neutron diffraction, and electrical resistivity measurements [12–15]. Besides, a cascade of magnetic

transformations appearing when cooling down and associated with the antiferro- and ferrimagnetic orderings of the several magnetic subsystems has been extensively studied by experimental methods and theoretical calculations [16–19].

The electronic and magnetic phase diagrams of oxy-/borates are complicated and permanently being updated. They are not restricted to iron compounds but include other  $Me = 3d$  metals. Under ambient pressure conditions several structure types, such as calcite ( $Me^{3+}BO_3$ ), warwickite ( $Me^{2+}Me^{3+}BO_4$ ), ludwigite ( $Me_2^{2+}Me^{3+}BO_5$ ), norbergite ( $Me_3^{3+}BO_6$ ), pyroborate ( $Me_2^{2+}B_2O_5$ ), and kotoite ( $Me_3^{2+}B_2O_6$ ), can be obtained within the ternary system  $Me-B-O$ :

$$\frac{1}{2}(2n \cdot MeO + m \cdot Me_2O_3 + p \cdot B_2O_3) \quad (1)$$

where parameters  $n$ ,  $m$ , and  $p$  correspond to the amounts of di- and trivalent metal, and boron ions per formula unit, respectively. Hence, the resultant oxy-/borate  $Me_n^{2+}Me_m^{3+}B_pO_{n+\frac{3}{2}(m+p)}$  could depend on its stoichiometry. One could expect that changing in  $n$ ,  $m$ , and  $p$  parameters could lead to new magnetic materials that are structurally linked to the

\* Corresponding author at: Laboratory of Physics of Magnetic Phenomena, Kirensky Institute of Physics, Akademgorodok 50, bld. 38, Krasnoyarsk 660036 Russia.  
E-mail address: [nat@iph.krasn.ru](mailto:nat@iph.krasn.ru) (N.V. Kazak).

known Fe oxy-/borates and thereby might possess potentially interesting physical properties. By analogy with the family of iron oxy-/borates  $Fe_n^{2+}Fe_m^{3+}B_pO_{n+\frac{3}{2}(m+p)}$ , it was proposed that  $Me = Ti$  [20], V [21,22], Mn [23–27], Co [26,27,28], Cr [21,29], Cu [30], and Ni [26] compounds could also form such families. Indeed, the newly-discovered orthoborate  $V_2BO_4$  [31] supplement the mixed-valence warwickite family. This material was found to show several anomalies in the temperature range 135–260 K associated with the crystallographic symmetry change and the transition to ferrimagnetic state at  $\sim 35$  K. The metaborate  $Co_4B_6O_{13}$  [32] recently added to the divalent cobalt oxyborates was reported to have an almost spinless ground state and a periodically undulating magnetization curve indicative of quantization of the total spin per spin tetrahedron. Fig. 1 presents a phase diagram of known structural types of 3d oxy-/borates within the ternary system (1). The left panel corresponds to the divalent oxy-/borates ( $m = 0$ ), while the right one includes both trivalent and mixed-valence compounds ( $m \neq 0$ ). It is obvious that far from all 3d metals form the borate polymorphs. It is also seen that the borate family containing the trivalent cobalt is restricted to just the ludwigite type and no other stoichiometry containing  $Co^{3+}$  ion was reported up to now. We have been unsuccessful in the synthesis of the cobalt calcite and warwickite phases and, hence, the stability of these structures is still under question. On the other hand, the substitution of trivalent ion by the higher valence ion  $m \cdot Me^{3+} = (m-1) \cdot Me^{2+} + Me^{m+2}$  makes it possible to obtain the samples with increasing concentration of ions of one own sort. The cobalt warwickites with tetravalent substitution  $Co_{1.5}Me_{0.5}BO_4$  ( $Me = Ti^{4+}, Zr^{4+}$ ) have been reported [33], but its physical properties were hitherto unknown. By going this way and careful choice of starting materials, we have synthesized a new oxyborate  $Co_{5/3}Nb_{1/3}BO_4$ , where the amount of  $Co^{2+}$  ions per formula unit is as large as 83%. The compound has been studied by a combination of single-crystal X-ray diffraction,  $dc$  magnetization, and specific heat measurements. The new oxyborate was found to crystallize in warwickite structure and exhibits intriguing magnetic behaviour that is not inherent in warwickites but has a strong resemblance to ludwigites, namely to  $Fe_3BO_5$ . The material undergoes two magnetic transitions: paramagnetic-antiferromagnetic at  $T_{N1} = 27$  K and antiferromagnetic-ferrimagnetic at  $T_{N2} = 14$  K. The clear signs of long-range magnetic order, manifesting both in the  $dc$  magnetization and specific heat measurements, make it a unique heterometallic oxyborate, which is in line with homometallic ones such as  $Mn_2BO_4$  ( $T_N = 23$  K) [23],  $V_2BO_4$  ( $T_N = 35$  K) [31],  $Fe_2BO_4$  ( $T_N = 150$  K) [13],  $Co_3BO_5$  ( $T_N = 42$  K) [18], and  $Fe_3BO_5$  ( $T_{N1} = 110$  K,  $T_{N2} = 70$  K) [14]. Results demonstrate a parallelism between cobalt and iron borate families.

## 2. Experimental techniques

Single crystals of  $Co_{5/3}Nb_{1/3}BO_4$  were grown using a flux method in the system  $Bi_2Mo_3O_{12} \cdot 3.63 \cdot B_2O_3 \cdot 0.7 \cdot Na_2O \cdot 5.97 \cdot CoO \cdot 0.31 \cdot Nb_2O_5$ . The flux was prepared in a platinum crucible ( $V = 100 \text{ cm}^3$ ) at a temperature

of 970 °C by sequential melting of powders: first,  $Bi_2Mo_3O_{12}$ ,  $B_2O_3$ , then  $Na_2CO_3$  was added in portions, after that  $CoO$  and  $Nb_2O_5$  were added in portions sequentially. The flux was homogenized at  $T = 1000$  °C for 3 h, then the temperature was first rapidly reduced to 970 °C and then slowly reduced at a rate of 4 °C/day. In two days, the crystal holder was extracted from the flux. The single crystals were separated by etching in a 20% aqueous solution of nitric acid.

Single crystals of  $Co_{5/3}Nb_{1/3}BO_4$  warwickite have a pronounced needle shape up to 5 mm long. The cross-section shows a very well defined planar face, which allows to position the crystal according to direction 1 and 2 as shown below in Fig. 1S of Supplemental Material [34]. The cross-section has a size of  $0.1 \times 0.2 \text{ mm}^2$ . The needle axis coincides with the  $c$ -axis of the crystal.

The X-ray diffraction patterns were collected from a single crystal at 296 K using the SMART APEX II single-crystal diffractometer (Bruker AXS) equipped with a PHOTON 2 CCD-detector, graphite monochromator, and Mo  $K\alpha$  radiation source. The structure was solved by direct methods [35] using the SHELXS program. The structure refinement was carried out by least-square minimization in the SHELXL program [36] using anisotropic thermal parameters of all atoms. The main information regarding crystal data, data collection, and refinement is reported in Table 1. The crystallographic data for the compound have been deposited with the Cambridge Crystallographic Data Centre, CCDC 2038293.

For magnetic measurements, one single crystal of 0.26 mg has been oriented and placed in the sample holder with the help of a microscope. The  $dc$  magnetization measurements were performed using a Quantum Design MPMS-XL. The sample was placed so that the needle axis was perpendicular (direction\_1 and direction\_2) and parallel (direction\_3) to the external magnetic field (Fig. 1S [34]).

The specific heat measurements were performed on single crystalline samples with an overall mass of 2.2 mg in the temperature range of 2–200 K using a commercial instrument (Quantum Design PPMS).

**Table 1**  
Crystallographic data and main parameters of processing and refinement  $Co_{5/3}Nb_{1/3}BO_4$ .

Crystal data	
$M_r$	113.32
Space group, Z	<i>Pbnm</i> (62), 8
Size, mm	$0.27 \times 0.07 \times 0.05$
T, K	296
$a$ , (Å)	9.3336(7)
$b$ , (Å)	9.4039(7)
$c$ , (Å)	3.1793(2)
$V$ , (Å <sup>3</sup> )	279.05(3)
$D_x$ , Mg/m <sup>3</sup>	4.864
$\mu$ , mm <sup>-1</sup>	11.063
Data collection	
Wavelength	Mo $K\alpha$ , $\lambda = 0.71073$ Å
Measured reflections	5484
Independent reflections	756
Reflections with $I > 2\sigma(I)$	673
Absorption correction	Multiscan
$R_{int}$	0.0452
$2\theta_{max}$ (°)	71.92
$h$	-15 → 15
$k$	-15 → 15
$l$	-5 → 5
Refinement	
$R[F^2 > 2\sigma(F^2)]$	0.0307
$wR(F^2)$	0.0738
$S$	1.139
Weight	$w = 1/[\sigma^2(F_o^2) + (0.0314P)^2 + 0.71P]$
Extinction	0.065(4)
$(\Delta/\sigma)_{max}$	0.00
$\Delta\rho_{max}$ , e/Å <sup>3</sup>	1.11
$\Delta\rho_{min}$ , e/Å <sup>3</sup>	-2.78

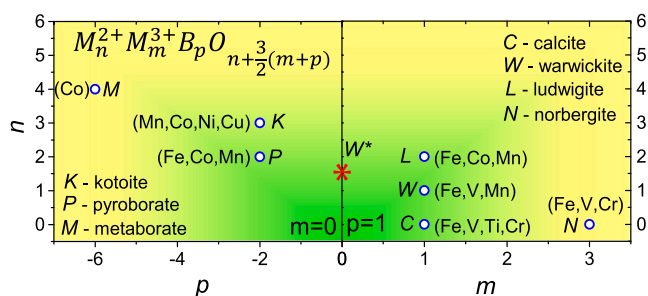


**Fig. 1.** The structural types diagram of transition metal oxy-/borates obtained within the ternary system M-B-O at ambient pressure. The parameters  $n$ ,  $m$ , and  $p$  are amounts of di-, trivalent metal ions and boron per formula unit. Red star denotes a new  $Co_{5/3}Nb_{1/3}BO_4$  warwickite.

### 3. Results and discussion

The crystal structure of  $\text{Co}_{5/3}\text{Nb}_{1/3}\text{BO}_4$  was solved and the stoichiometry was confirmed. The compound was established to adopt the orthorhombic structure with  $Pbmm$  space group. The unit cell parameters are  $a = 9.3336(7) \text{ \AA}$ ,  $b = 9.4039(7) \text{ \AA}$ ,  $c = 3.1793(2) \text{ \AA}$ ,  $V = 279.05(3) \text{ \AA}^3$ , and  $Z = 8$ . The crystal structure has two crystallographically non-equivalent metal sites M1 and M2, which are octahedrally-coordinated (Fig. 2). The M1 site is occupied by Co and Nb ions with the ratio 0.66/0.34, while the M2 site is filled by Co ions (Table 2). By analyzing the M–O bond distances (Table 3) we established that both octahedra are compressed along the main axis with an average bond length  $\langle \text{M1-O} \rangle = 2.088(2) \text{ \AA}$  and  $\langle \text{M2-O} \rangle = 2.109(2) \text{ \AA}$ . The octahedral distortions were estimated through the main component of electric field gradient tensor  $V_{zz}$  similarly as it was done for other oxyborates [23,37]. The distortion parameters are  $V_{zz}(1) = 0.16 \text{ e/\AA}^3$  and  $V_{zz}(2) = 0.08 \text{ e/\AA}^3$ , for  $\text{M1O}_6$  and  $\text{M2O}_6$  octahedra, respectively. So, the  $\text{M1O}_6$  octahedron is smaller and more distorted. Using a bond valence sums (BVS) [38] method the average oxidation states for Co ions occupying M1 and M2 sites were calculated to be +2.13 and +1.99, respectively. The same BVS analysis for Nb and B ions gives the value of +3.80 and +2.95, respectively. Thus, we conclude that the spacious M2 site is exclusively occupied by  $\text{Co}^{2+}$  ions. Taking into account the Nb ion distribution determined by single-crystal X-ray diffraction the oxidation state of M1 metal site was found to be +2.7, which is close to +3 expected from the general formula of the warwickite. This is in line with the conclusion that in warwickites the structure is only stable when the size of the divalent cation  $\text{Me}^{2+}$  at M2 site is larger than that one of the trivalent  $\text{Me}^{3+}$  at M1 site [39]. Although there is a large ionic-size mismatch between HS  $\text{Co}^{2+}$  (0.745  $\text{ \AA}$ ) and  $\text{Nb}^{5+}$  (0.64  $\text{ \AA}$ ), whereas ionic radius of LS  $\text{Co}^{2+}$  is 0.65  $\text{ \AA}$  [40], we conjecture that  $\text{Co}^{2+}$  ions adopt a HS state. This conclusion is supported by its large abundance in oxyborates as compared to LS  $\text{Co}^{2+}$ , and the subsequent analysis of magnetic properties (see Table 5 and text below).

We examined the magnetic properties of the new oxyborate by  $dc$  magnetization measurements. An external magnetic field was directed in  $ab$ -plane ( $dir_1$  and  $dir_2$ ) and along the  $c$ -axis ( $dir_3$ ). Field-cooled (FC) and zero-field-cooled (ZFC)  $dc$  magnetizations measured as a function of the temperature with an applied field of 600 Oe at different crystal orientations are shown in Fig. 3. First we want to note that the magnetization of  $\text{Co}_{5/3}\text{Nb}_{1/3}\text{BO}_4$  demonstrates a high anisotropy. The magnetization along the  $c$ -axis is 100 times lower than those obtained for directions in the  $ab$ -plane, where the difference between magnetic moments measured in-plane is about 20%. This clearly indicates that the  $c$ -axis is a hard magnetization direction. Next, the magnetization measurements of  $\text{Co}_{5/3}\text{Nb}_{1/3}\text{BO}_4$  reveal two magnetic transitions. As Fig. 3 and its inset demonstrate, the maximum in the magnetization at  $T_{N1} = 27 \text{ K}$  evidences an antiferromagnetic transition. A broad susceptibility

**Table 2**

Coordinates of atoms, occupancy and equivalent isotropic displacement parameters of  $\text{Co}_{5/3}\text{Nb}_{1/3}\text{BO}_4$ .

	x	y	z	Ueq	S.O.F.
Co1	0.07608(5)	0.11423(5)	0.2500	0.01571(14)	0.656(9)
Nb1	0.07608(5)	0.11422(5)	0.2500	0.01571(14)	0.344(9)
Co2	0.18185(5)	0.40016(4)	0.7500	0.01041(13)	
O1	0.2466(2)	0.2531(2)	0.2500	0.0107(4)	
O2	0.3847(3)	0.4875(3)	0.7500	0.0122(4)	
O3	0.0044(3)	0.2599(2)	0.7500	0.0129(4)	
O4	0.3626(4)	0.0295(3)	0.2500	0.0205(6)	
B	0.3718(4)	0.1739(4)	0.2500	0.0090(5)	

**Table 3**

Main bond lengths of  $\text{Co}_{5/3}\text{Nb}_{1/3}\text{BO}_4$ .

bond	distance ( $\text{ \AA}$ )	bond	distance ( $\text{ \AA}$ )	bond	distance ( $\text{ \AA}$ )
Co1 Nb1—O2 <sup>i</sup>	2.0201(15)	Co2—O4 <sup>viii</sup>	2.0440(17)	B—O3 <sup>xi</sup>	1.386(4)
Co1 Nb1—O2 <sup>ii</sup>	2.0201(15)	Co2—O4 <sup>ix</sup>	2.0440(17)	B—O4	1.361(4)
Co1 Nb1—O2 <sup>iii</sup>	2.027(3)	Co2—O2	2.064(2)	B—O1	1.386(4)
Co1 Nb1—O1	2.059(2)	Co2—O3	2.117(2)		
Co1 Nb1—O3 <sup>iv</sup>	2.2021(16)	Co2—O1	2.1917(16)		
Co1 Nb1—O3	2.2022(16)	Co2—O1 <sup>vii</sup>	2.1917(16)		

upturn below  $T_{N2} = 14 \text{ K}$  evidences spin canting or some other ferro- or ferrimagnetic transition. Below  $T_{N2}$ , FC magnetization steadily increases on cooling and the ZFC drops to zero, being peaklike. For  $dir_1$ , we have additionally measured the magnetization at 50 Oe, 5 kOe, and 50 kOe (Fig. 4). A close examination in a weak field reveals another one anomaly that looks like a broad maximum at 20 K, which is then hidden by the growing magnetic moment induced by a magnetic transition at  $T_{N2}$ . In fact, the transition at  $T_{N2}$  is so sharp that in the fields of 5 kOe and above this anomaly is not visible. The observed temperature dependence of the magnetization is not in accord with ordinary antiferromagnetism but reflects a complex ferrimagnetic ordering of  $\text{Co}^{2+}$  magnetic moments with the magnetic sublattices, which possess magnetizations non-equivalent in magnitude and temperature rate.

The average susceptibility  $\chi_{av}(T) = \frac{\chi_{dir_1} + \chi_{dir_2} + \chi_{dir_3}}{3}$ , measured at  $H = 50 \text{ kOe}$ , follows above 100 K quite well the Curie-Weiss law (Fig. 5):

$$\chi(T) = \chi_0 + \frac{C}{T - \theta} \quad (2)$$

where  $\chi_0$  is the temperature independent term,  $C$  is the Curie-Weiss constant, and  $\theta$  is the Curie-Weiss temperature. We note that for  $T > 100 \text{ K}$ ,  $M(H)$  is linear up to 50 kOe, so the susceptibility may be calculated as  $\chi = M(H)/H$  at 50 kOe. The fits along the three directions and on the average susceptibility are given in Table 4. It is evidenced that the paramagnetic phase is highly anisotropic, with an

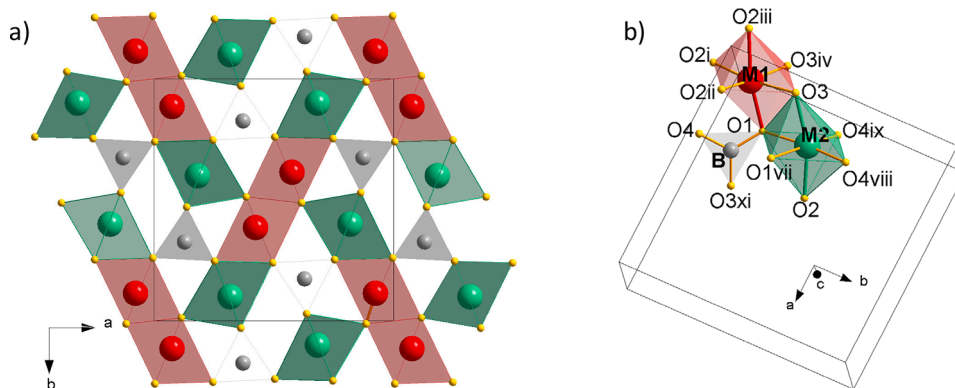


**Fig. 2.** a) The crystal structure of new oxyborate projected in  $ab$ -plane. The non-equivalent metal sites M1 and M2 are highlighted by red and green, respectively. The  $\text{BO}_3$  groups are depicted by grey triangles. b) Metal and boron coordinations. The main octahedral axes as shown by red and green for M1 and M2 sites, respectively.

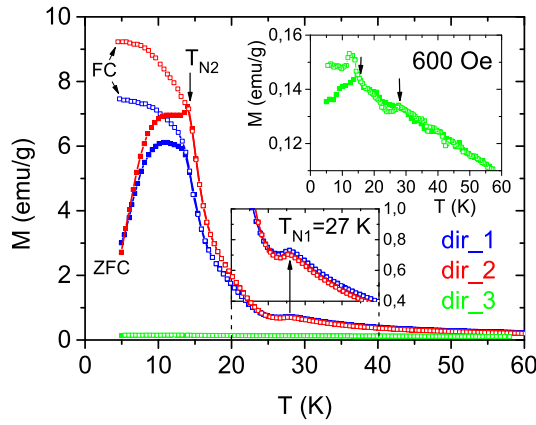


**Fig. 3.** Magnetization vs. temperature of  $\text{Co}_{5/3}\text{Nb}_{1/3}\text{BO}_4$  single crystal at the field 600 Oe applied in  $ab$ -plane ( $\text{dir}_1$ ,  $\text{dir}_2$ ) and along  $c$ -axis ( $\text{dir}_3$ ). The filled and empty symbols denote ZFC and FC regimes. Top inset shows strongly reduced magnetic moment along  $c$ -axis in zoom. Bottom inset is the enlarge plot of  $M(T)$  near magnetic transition at  $T_{N1}$ . Arrows show an onset of magnetic transitions.

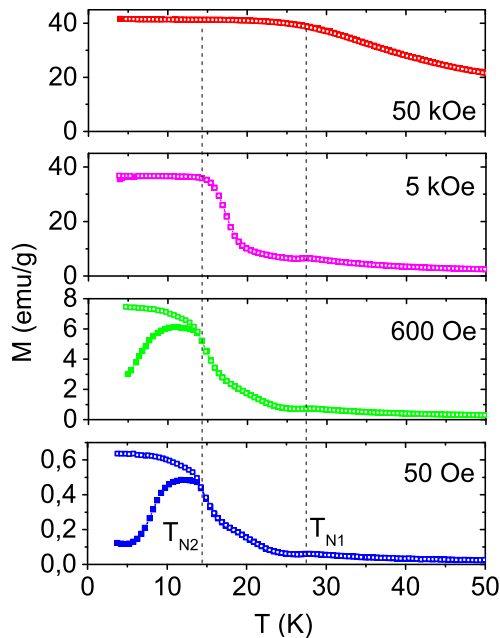


**Fig. 4.** The temperature dependencies of the magnetizations a  $\text{Co}_{5/3}\text{Nb}_{1/3}\text{BO}_4$  single crystal measured at different fields applied in  $ab$ -plane (direction 1). The plot shows a sharp increase in magnetic moment below  $T_{N2}$ .

$ab$  easy plane anisotropy. Note, that the magnetic anisotropy observed in  $\text{Co}_{5/3}\text{Nb}_{1/3}\text{BO}_4$  is the highest among those found in other warwickites  $\text{Mn}_2\text{BO}_4$  [23]  $\text{Mn}_{2-x}\text{Mg}_x\text{BO}_4$  [41],  $\text{Mn}_{2-x}\text{Fe}_x\text{BO}_4$  [42],  $\text{Mg}_{1-x}\text{Co}_x\text{FeBO}_4$  [43]. In fact, the anisotropy in  $\text{Co}_{5/3}\text{Nb}_{1/3}\text{BO}_4$  is comparable with that we reported for  $\text{Fe}_3\text{BO}_5$  and  $\text{Co}_3\text{BO}_5$  ludwigites [18].

The constant  $\chi_0 = 1.6 \cdot 10^{-3}$  emu/mol and the parameter  $\theta_{av} = -8.9$  K were found. It is important to remark that the sign of the obtained in the individual fits is not indicative of the ferro or antiferro magnetic character of interactions along that direction, since this parameter includes an anisotropic contribution [44]. The negative sign of  $\theta_{av}$  points to an average antiferromagnetic exchange interactions between  $\text{Co}^{2+}$ . Most heterometallic warwickites studied up to now show high negative Curie-Weiss temperatures and rather low magnetic transition temperatures. For instance,  $\theta$  was found to be  $-450$  K ( $\text{NiFeBO}_4$ ) [45],  $-315$  K

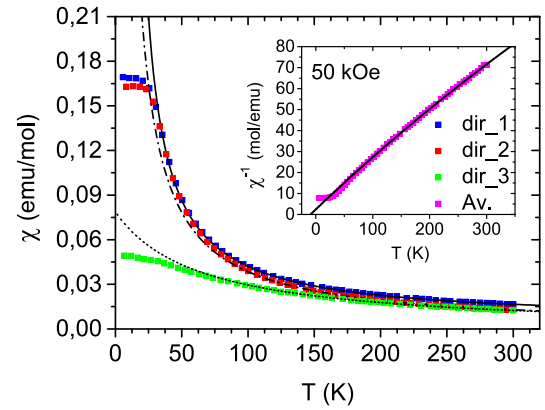


**Fig. 5.** Magnetic susceptibility for  $\text{Co}_{5/3}\text{Nb}_{1/3}\text{BO}_4$  single crystal as a function of temperature in applied field of 50 kOe oriented in  $ab$ -plane ( $\text{dir}_1$  and  $\text{dir}_2$ ) and along  $c$ -axis ( $\text{dir}_3$ ). The inset shows the inverse average susceptibility ( $\text{Av.}$ ). The experimental data are shown by symbols, while dotted, dashed and solid lines denote fitting using Eq.1.

**Table 4**

Magnetic parameters of  $\text{Co}_{5/3}\text{Nb}_{1/3}\text{BO}_4$  extracted in the paramagnetic phase.

	$\chi_0$ (emu/mol)	C (emu·K/mol)	$\theta$ (K)	$\mu_{\text{eff}}$ ( $\mu_B/\text{f.u.}$ )
$\text{dir}_1$	$4.9 \pm 0.1 \cdot 10^{-3}$	$3.38 \pm 0.02$	$8.7 \pm 0.5$	$5.2 \pm 0.1$
$\text{dir}_2$	$0.9 \pm 0.1 \cdot 10^{-3}$	$3.51 \pm 0.02$	$7.8 \pm 0.4$	$5.3 \pm 0.1$
$\text{dir}_3$	$0.0 \pm 0.5 \cdot 10^{-3}$	$4.6 \pm 0.2$	$-54 \pm 6$	$6.1 \pm 0.1$
average	$1.6 \pm 0.2 \cdot 10^{-3}$	$3.81 \pm 0.08$	$-8.9 \pm 2.4$	$5.52 \pm 0.06$

( $\text{CoFeBO}_4$ ) [43], and  $-283$  K ( $\text{MgFeBO}_4$ ) [43], while  $T_{\text{SG}} = 12, 22$ , and  $10$  K, respectively. As a result, the majority of the warwickites of interest exhibit huge magnetic frustrations with empirical parameter  $\eta = |\theta|/T_{\text{SG}}$  ranging from 8 to 37 [43]. We estimated the impact of the magnetic frustrations in  $\text{Co}_{5/3}\text{Nb}_{1/3}\text{BO}_4$  through an average Curie-Weiss temperature  $\theta_{av}$ , obtained using  $\chi_{av}(T)$ . One obtains  $\eta = |\theta_{av}|/T_{N1} = 0.33$  that indicates minority frustrations and is consistent with the onset of long-range magnetic order. Actually, the  $\eta$  value found for  $\text{Co}_{5/3}\text{Nb}_{1/3}\text{BO}_4$  is the smallest among known warwickites including homometallic  $\text{Fe}_2\text{BO}_4$  [13] and  $\text{Mn}_2\text{BO}_4$  [23]. Therefore, this warwickite is different than those behaving as spin-glasses, while it resembles some Co containing ludwigites that show one or more long range order transitions. For example, in  $\text{Co}_{3-x}\text{Fe}_x\text{BO}_5$ , the compounds with  $x = 0, 0.75$  and  $1$  have  $\theta$ 's lower than  $T_c(T_{N2})$  [18]. It can be expected for compounds exhibiting complicated magnetic sublattices and competing interactions, and in some cases giving rise to sequential magnetic transitions with different characters (ferro-, ferri-, or antiferromagnetic), as is the present  $\text{Co}_{5/3}\text{Nb}_{1/3}\text{BO}_4$  warwickite.

Note that the average magnetic susceptibility in the field of 50 kOe is about  $\chi_{av}(4.2 \text{ K}) = 1.26 \cdot 10^{-1}$  emu/mol =  $62 \cdot 10^{-5}$  emu/gOe which is one order higher than that reported for polycrystalline  $\text{Fe}_2\text{BO}_4$  at similar conditions ( $8.54 \cdot 10^{-5}$  emu/gOe) [13]. This behavior implies the enhancement of the ferrimagnetism in  $\text{Co}_{5/3}\text{Nb}_{1/3}\text{BO}_4$ , which is probably originated from the difference in the moduli and orientations of the magnetization sublattices.

The average Curie-Weiss constant  $C_{av} = 3.81$  emu·K/mol corresponds to an effective magnetic moment  $\mu_{\text{eff}} = 5.52 \mu_B/\text{f.u.}$  or  $4.28 \mu_B$  per  $\text{Co}^{2+}$  ion, while the value obtained for  $\text{Co}^{2+}$  ion ( $S = 3/2$ ) for a spin-only magnetic moment with  $g = 2$  is  $3.87 \mu_B$ . One can conclude that in  $\text{Co}_{5/3}\text{Nb}_{1/3}\text{BO}_4$  warwickite the  $\text{Co}^{2+}$  ions are a high-spin state and have a higher value of magnetic moment due to the orbital contribution, which is very typical for octahedrally coordinated  $\text{Co}^{2+}$ . Putting the effective magnetic moment of  $\text{Co}^{2+}$  ion  $\mu_{\text{eff}}/\text{Co} =$

$$\sqrt{(g_{\text{Co}^{2+}})^2 \cdot S \cdot (S + 1)},$$



moment corresponds to  $g_{Co^{2+}} = 2.2$ , which is in accord with the usually observed value for  $Co^{2+}$  ion in octahedral coordination. Noteworthy, that value of  $\mu_{eff}$  for  $Co_{5/3}Nb_{1/3}BO_4$  is extremely close to that extracted in a similar way for  $Co_3BO_5$  ludwigite,  $\mu_{eff} = 4.0 \mu_B$  per  $Co^{2+}$  ion, where the  $Co^{2+}$  ions are assumed to be in a high-spin state, while the  $Co^{3+}$  ion is in a low-spin state. We also note that the experimentally observed value of  $\mu_{eff}$  for  $Co_{5/3}Nb_{1/3}BO_4$  is comparable to those found for other borate systems containing divalent cobalt (Table 5).

To gain further insight into the magnetism of  $Co_{5/3}Nb_{1/3}BO_4$ , the isothermal magnetization curves were measured. Fig. 6 shows  $M(H)$  curves obtained for the applied magnetic field in *ab*-plane (*dir*\_1). A hysteresis cycle at  $T = 4.2$  K is an intrinsic sign of a ferro- or ferrimagnetic state (Fig. 6a). The magnetization tends to the saturation at high fields. The saturation moment obtained by linear extrapolation of the high-field magnetization data to zero field yields  $M_s(4.2 \text{ K}) = 1.27 \mu_B/\text{f.u.}$ . The remanent magnetization  $M_r = 0.47 \mu_B/\text{f.u.}$  is only 37% of the  $M_s$ . The coercive field  $H_C(4.2 \text{ K}) = 1 \text{ kOe}$ . As the compound is heated the magnetization curve is drastically modified. Although the  $M_s$  remains almost constant, the coercive field rapidly decreases down to 150 Oe at 10 K and becomes zero at 20 K (Fig. 6b,c). At the same temperature, which is in temperature range  $T_{N2} < T < T_{N1}$ , the magnetization curve shows zero magnetic remanence and a complex shape reflecting the magnetization process of the magnetic sublattices (Fig. 6c). Finally, at  $T > T_{N1}$  the material exhibits a paramagnetic behavior (Fig. 6d).

The saturation magnetic moment as a function of temperature shows a monotonic decrease (Fig. 7a). Above  $T_{N1} = 27$  K, the non-zero  $M_s$  tail reflects short range correlations. The antiferromagnetic susceptibility  $\chi_{AFM}(T)$  determined from the high-field slope of the  $M(H)$  curves is typical for an antiferromagnet measured along the parallel direction (Fig. 7b). The first derivative of  $\frac{d\chi_{AFM}(T)}{dT}$  has a maximum at the temperature corresponding to  $T_{N1}$ .

The saturation magnetic moment is rather small compared to that expected  $\sim 5 \mu_B$ . The drastic reduction of the moment can be explained by the partial compensation due to a ferrimagnetic arrangement of Co moments. A naive accounting of the magnetization per formula unit for fully antiparallel spin arrangement yields of  $M_1 = |-1.86|$  and  $M_2 = 3.13 \mu_B$  for the simplest model of the two-sublattice ferrimagnet. Assuming that  $M_{1,2} = n_{1,2}gS\mu_B$  are magnetic sublattices associated with crystallographically non-equivalent metal sites,  $S = 3/2$  is a spin value for  $Co^{2+}$ , and  $g = 2$  for spin magnetism, the obtained concentrations of  $Co^{2+}$  ions at  $M_1$  and  $M_2$  sites equal  $n_{1,2} = 0.62$  and  $1.04$ , respectively. These values are in good agreement with the site occupation factors obtained from single-crystal X-ray diffraction (Table 2). Thus, the presented data are consistent with a collinear order of the one up-spin and two-thirds down-spin  $d^7$  ions ( $Co^{2+}$ ), leading to a resultant magnetization of  $1.27 \mu_B/\text{f.u.}$

Additionally, the hysteresis cycles for the second direction of the magnetic field in *ab*-plane (*dir*\_2) as well as along the *c*-axis (*dir*\_3) were measured carefully (Fig. 7c), which confirm a high anisotropy of  $Co_{5/3}Nb_{1/3}BO_4$  single crystal. In the *c*-direction the magnetization shows no hysteresis, with linear  $M(H)$  curves at all measured temperatures. The magnetization curves measured in *ab*-plane (*dir*\_1 and *dir*\_2) behave similar, without showing a noticeable difference in the magnitude.

The temperature-dependent measurements of specific heat  $C_p$  of  $Co_{5/3}Nb_{1/3}BO_4$  have revealed two clear anomalies at  $T_{N1} = 27$  K and  $T_{N2} = 14$  K, which are in excellent agreement with the magnetization data (Fig. 8a). The anomaly at  $T_{N1}$  is a  $\lambda$ -type indicating a second-order phase transition, while the second one at  $T_{N2}$  has a broader shape. In the

magnetic field, both anomalies smear out and are shifted to higher temperatures. At  $T = 200$  K, the specific heat  $C_p = 100.7 \text{ J/mol K}$  does not reach the thermodynamic limit  $3Rz = 174.5 \text{ J/mol K}$  of the lattice contribution, with  $R$  being the gas constant and  $z$  the number of ions per unit cell. The anomalous contribution of the specific heat  $\Delta C_p$  was estimated using the Debye-Einstein approximation similar to the procedure applied for  $Mn_2BO_4$  and  $Co_3BO_5$  oxyborates [23,46]. The temperatures far from anomalous regions were fitted. The Debye temperature was obtained to be  $\Theta_D = 356 \pm 20$  K. This value is in good agreement with those of 512 K ( $Mn_2BO_4$  [23]), 360 K ( $V_2BO_4$  [31]), and 493 K ( $Co_3BO_5$  [46]). The low-temperature part of the total entropy  $\Delta S$  saturates at about 100 K, reaching approximately  $10.1 \text{ J/mol K}$  (Fig. 8b). The entropy released at magnetic transition amounts to  $\Delta S(T_{N1}) = 4.5 \pm 0.5 \text{ J/mol K}$  that is about 42% of saturation value. This value ( $\Delta S \approx 10 \text{ J/mol K}$ ) is very close to  $\Delta S = 9.6 \text{ J/mol K}$  which corresponds to the transition being caused by the coupling of the ground Kramers doublets for the  $Co^{2+}$  ions, since the next excited doublet is at much higher energy and cannot be thermally populated, i.e.  $\Delta S = R \cdot n_{Co^{2+}} \cdot \ln 2$ . Besides, the critical entropy can be compared to the value  $\Delta S(T_N) = 8.30 \pm 1.6 \text{ J/mol K}$  for  $Co_3BO_5$  where two high-spin  $Co^{2+}$  ions are assumed to contribute to the entropy at the magnetic transition [46].

So, we can conclude that the  $Co_{5/3}Nb_{1/3}BO_4$  warwickite undergoes two magnetic transitions: the paramagnetic-antiferromagnetic at  $T_{N1} = 27$  K and antiferro-ferrimagnetic at  $T_{N2} = 14$  K. The abrupt growth in the *dc* magnetization below  $T_{N2}$  (in Fig. 3) correlates with this assumption. Neutron diffraction will be needed to confirm the spin orders below  $T_{N1}$  and  $T_{N2}$  transitions. Noteworthy is the strong similarity of the magnetic behavior of a new oxyborate with that of Fe and Co ludwigites. It is well known that  $Fe_3BO_5$  exhibits two magnetic transitions: at  $T_{N1} = 110$  K the magnetic moments belonging to M4-M2-M4 triads are ordered antiferromagnetically along *a*-axis, while at  $T_{N2} = 70$  K magnetic moments of M3-M1-M3 triads are ordered ferrimagnetically along *b*-axis [14,18]. (Here, M1, M2, M3, and M4 are numbers of crystallographically non-equivalent metal sites in ludwigite structure). Unlike iron ludwigite,  $Co_3BO_5$  demonstrates only one magnetic transition to the ferrimagnetic state at  $T_N = 42$  K, which is proposed to associated with the ordering of  $Co^{2+}$  magnetic moments belonging to M1, M2, and M3 sites whereas the  $Co^{3+}$  ions located at M4 site are assumed in a low-spin state [46]. The second transition becomes manifested if LS  $Co^{3+}$  ions are replaced by HS  $Fe^{3+}$  ions [50]. As a result,  $Co_2FeBO_5$  shows two magnetic transitions similar to Fe ludwigite [14,18]. In  $Co_{5/3}Nb_{1/3}BO_4$  these two transitions although strongly shifted to the lower temperatures manifest themselves both in the magnetic and specific heat measurements indicating the common peculiarities of the magnetic ground state forming in warwickites and ludwigites.

#### 4. Conclusions

By the changing in the stoichiometry of the oxy-/borates  $Me_n^{2+}Me_m^{3+}B_pO_{n+\frac{3}{2}(m+p)}$  and using a pentavalent substitution, we have obtained a new cobalt compound  $Co_{5/3}Nb_{1/3}BO_4$ , in which the concentration of  $Co^{2+}$  ions per formula unit reaches 83%, contributing to the magnetism of the system. The single crystals were found to crystallize in the warwickite structure with space group  $Pbnm$ . The  $Co^{2+}/Nb^{5+}$  ions share the octahedral M1 site and the  $Co^{2+}$  ions fill exclusively the M2 site. The magnetic properties were studied through the *dc* magnetization measurements at applied fields along the

Table 5

The effective magnetic moments experimentally observed for different oxy-/borates containing divalent cobalt ions.

	$Co_{5/3}Nb_{1/3}BO_4$ [p.w.]	$Co_3BO_5$ [46]	$Co_2B_2O_5$ [27]	$Co_3B_2O_6$ [47]	$Co_4B_6O_{13}$ [32]	$\alpha-CoB_4O_7$ [48]	$SrCo_2BPO_7$ [49]
$\mu_{eff} (\mu_B/Co^{2+})$	4.28	4.0*	4.96	4.92	4.90	5.00	5.00

\* The effective magnetic moment is obtained assuming that  $Co^{2+}$  ions are in high-spin state, and  $Co^{3+}$  ions are in low-spin state.

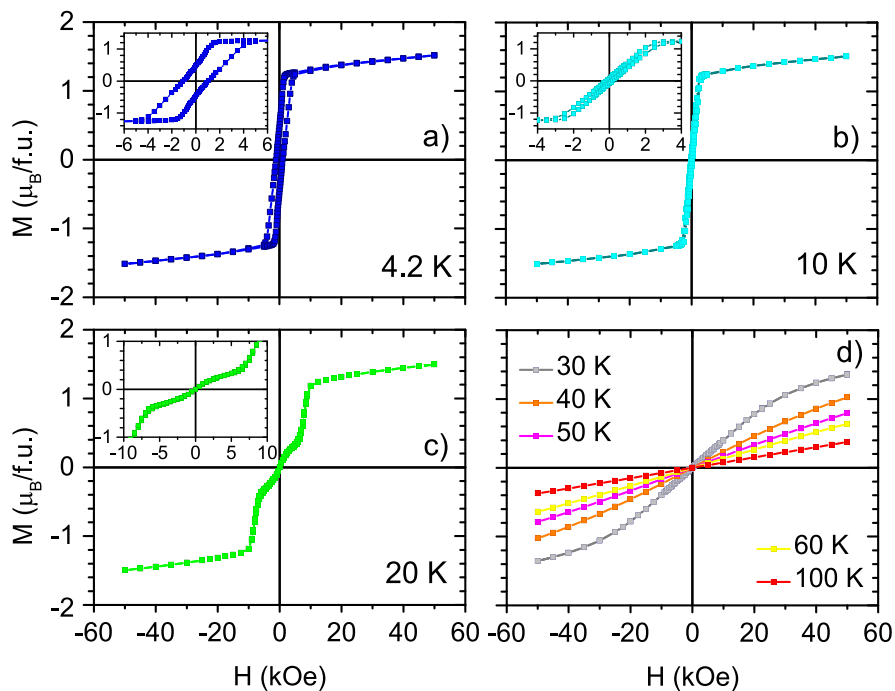


Fig. 6. Field dependences of the magnetization measured at temperature range of 4.2–100 K. The insets are low-field magnetization curves showing the transformation of the hysteresis loop upon heating.

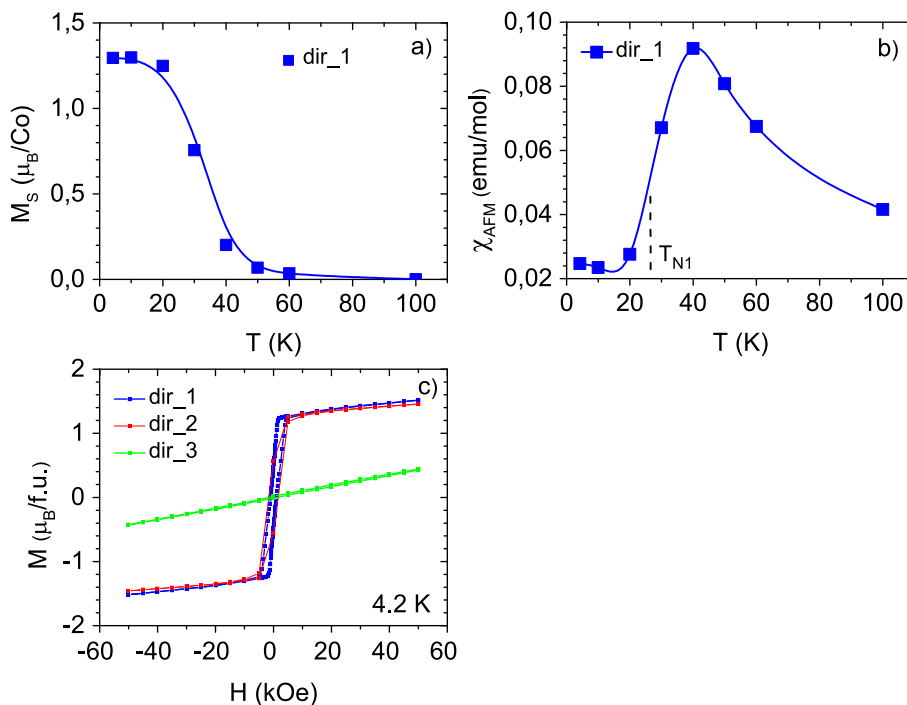
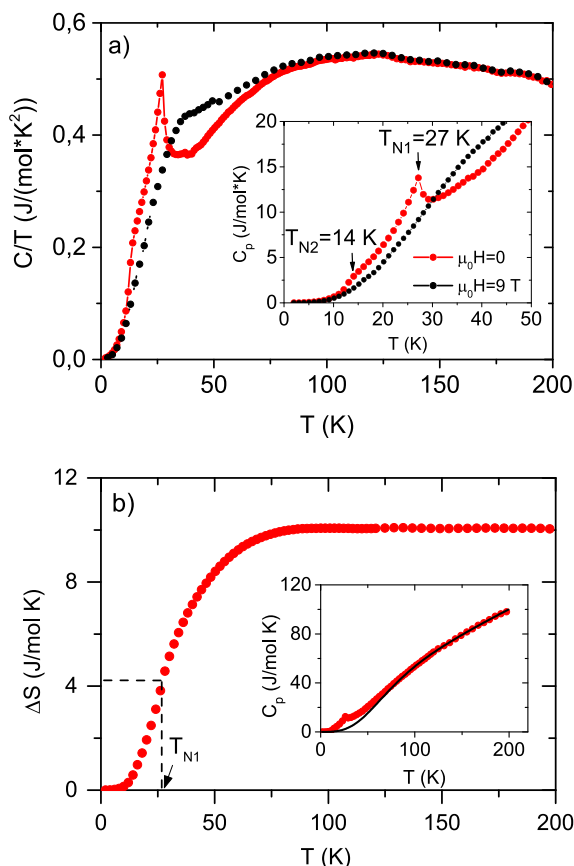


Fig. 7. a) The experimental saturation magnetic moment ( $\mu_B/\text{Co}$ ) vs temperature for  $\text{Co}_{5/3}\text{Nb}_{1/3}\text{BO}_4$  (blue symbols); guide to the eye (solid curve). b) An antiferromagnetic susceptibility  $\chi_{AFM}(T)$ , determined from the high-field slope of the  $M(H)$  cycles (blue symbols). The dashed line corresponds to the maximum of the first derivative  $\frac{d\chi_{AFM}(T)}{dT}$  showing the onset of antiferromagnetic ordering at  $T_{N1} = 27$  K. c) Hysteresis cycles at  $T = 4.2$  K for applied field in  $ab$ -plane and  $c$ -axis.

crystallographic  $c$ -axis and in the  $ab$ -plane. New oxyborate was found to exhibit two magnetic transitions at  $T_{N1} = 27$  K and  $T_{N2} = 14$  K. First of them is associated with a long-range antiferromagnetic ordering of  $\text{Co}^{2+}$  magnetic moments, while the second has a ferrimagnetic origin. In the temperature range  $T_{N2} < T < T_{N1}$  a magnetization curve shows a complex shape without any remanent magnetization. Below  $T_{N2}$  the hysteresis cycle is opened with the net moment  $1.27 \mu_B/\text{f.u.}$  originated from

magnetic moments of different modulus and orientation. The  $c$ -axis was found to be a hard magnetization direction. The specific heat measurements were revealed two magnetic anomalies in accordance with magnetic measurements. The magnetic behavior of  $\text{Co}_{5/3}\text{Nb}_{1/3}\text{BO}_4$  warwickite is straightly similar to that of ludwigites. It is evident, these materials have strong structural and magnetic affinities.



**Fig. 8.** a) Specific heat data for  $\text{Co}_{0.5/3}\text{Nb}_{1/3}\text{BO}_4$  in  $C_p/T$  vs  $T$  representation measured under zero and 9 T applied fields. The inset: the temperature dependent  $C_p$  showing evidence of two anomalies associated with magnetic transitions at  $T_{N1}$  and  $T_{N2}$ . b) Entropy as a function of temperature. The dashed lines indicate the entropy released at magnetic transition  $T_{N1}$ . The inset shows experimental specific heat (red points) and the lattice contribution obtained by fitting to Debye-Einstein approximation.

#### CRediT authorship contribution statement

**N.V. Kazak:** Conceptualization, Methodology, Funding acquisition. **N.A. Belskaya:** Data curation, Investigation. **E.M. Moshkina:** Data curation, Investigation. **L.N. Bezmaternykh:** Investigation, Methodology. **A.D. Vasiliev:** Investigation. **J. Bartolome:** Data curation, Investigation. **A. Arauzo:** Data curation, Investigation. **D.A. Velikanov:** Data curation, Investigation. **S.Yu. Gavrilkin:** . **M.V. Gorev:** Data curation, Investigation. **G.S. Patrino:** Data curation, Investigation. **S.G. Ovchinnikov:** Supervision.

#### Declaration of Competing Interest

The authors declare that they have no known competing financial interests or personal relationships that could have appeared to influence the work reported in this paper.

#### Acknowledgments

The authors acknowledge M. Molokeev for the orientating the single crystal for magnetic measurements. The X-ray diffraction and specific heat measurements were carried out in the Common Access Facility Centres of SB RAS (Krasnoyarsk, Russia) and P.N. Lebedev Physical Institute of RAS (Moscow, Russia). This work has been financed by the Russian Foundation for Basic Research (project no. 20-02-00559). We acknowledge financial support from the Spanish MINECO DWARFS

project MAT2017-83468-R and Gobierno de Aragón (Group, E12-20R).

#### Appendix A. Supplementary data

Supplementary data to this article can be found online at <https://doi.org/10.1016/j.jmmm.2021.168056>.

#### References

- [1] H.F.J. Glass, Z. Liu, P.M. Bayley, E. Suard, S.-H. Bo, P.G. Khalifah, C.P. Grey, S. E. Dutton,  $\text{Mg}_x\text{Mn}_{2-x}\text{B}_2\text{O}_5$  Pyroborates ( $2/3 \leq x \leq 4/3$ ): High Capacity and High Rate Cathodes for Li-Ion Batteries, *Chem. Mat.* 29 (7) (2017) 3118–3125, <https://doi.org/10.1021/acs.chemmater.7b00177>.
- [2] H. Chen, B.B. Xu, Q.S. Ping, B.Z. Wu, X.K. Wu, Q.Q. Zhuang, et al.,  $\text{Co}_2\text{B}_2\text{O}_5$  as an anode material with high capacity for sodium ion batteries, *Rare Met.* 39 (9) (2020) 1045–1052, <https://doi.org/10.1007/s12598-020-01383-8>.
- [3] B. Xu, Y. Liu, J. Tian, X. Ma, Q. Ping, B. Wang, Y. Xia,  $\text{Ni}_3(\text{BO}_3)_2$  as anode material with high capacity and excellent rate performance for sodium-ion batteries, *Chem. Eng. J.* 363 (2019) 285–291, <https://doi.org/10.1016/j.ccej.2019.01.089>.
- [4] M. Dong, Q. Kuang, X. Zeng, L. Chen, J. Zhu, Q. Fan, Y. Zhao, Mixed-metal borate  $\text{FeVBO}_4$  of tunnel structure: Synthesis and electrochemical properties in lithium and sodium ion batteries, *J. Alloys Compd* 812 (2020), 152165, <https://doi.org/10.1016/j.jallcom.2019.152165>.
- [5] V. Pralong, B. Le Roux, S. Malo, A. Guesdon, F. Lainé, J.F. Colin, C. Martin, Electrochemical activity in oxyborates toward lithium, *J. Solid State Chem.* 255 (2017) 167–171, <https://doi.org/10.1016/j.jssc.2017.08.010>.
- [6] I. Bernal, C.W. Struck, J.G. White, New transition metal borates with the calcite structure, *Acta Crystallogr.* 16 (1963) 849–850, <https://doi.org/10.1107/S0365110X63002255>.
- [7] I.S. Edel'man, A.V. Malakhovskii, T.I. Vasil'eva, V.N. Seleznev, *Sov. Phys. Solid State* 14 (1972) 2442.
- [8] V.A. Sarkisyan, I.A. Troyan, I.S. Lyubutin, A.G. Gavriluk, A.F. Kashuba, Magnetic collapse and the change of electronic structure of  $\text{FeBO}_3$  antiferromagnet under high pressure, *JETP Lett.* 76 (2002) 664–669, <https://doi.org/10.1134/1.1545580>.
- [9] I.A. Troyan, M.I. Eremets, A.G. Gavriluk, I.S. Lyubutin, V.A. Sarkisyan, Transport and optical properties of iron borate  $\text{FeBO}_3$  under high pressures, *JETP Lett.* 78 (2003) 13–16, <https://doi.org/10.1134/1.1609568>.
- [10] J.P. Attfield, A.M.T. Bell, L.M. Rodriguez-Martinez, J.M. Grenèche, R.J. Cernik, J. F. Clarke, D.A. Perkins, Electrostatically driven charge-ordering in  $\text{Fe}_2\text{OBO}_3$ , *Nature* 396 (1998) 655–658, <https://doi.org/10.1038/25309>.
- [11] M. Mir, R.B. Guimaraes, J.C. Fernandes, M.A. Continentino, A.C. Doriguetto, Y. P. Mascarenhas, L. Ghivelder, Structural Transition and Pair Formation in  $\text{Fe}_2\text{O}_2\text{BO}_3$ , *Phys. Rev. Lett.* 87 (2001), 147201, <https://doi.org/10.1103/PhysRevLett.87.147201>.
- [12] M. Angst, R.P. Hermann, W. Schweika, J.-W. Kim, P. Khalifah, H.J. Xiang, D. Mandrus, Incommensurate Charge Order Phase in  $\text{Fe}_2\text{OBO}_3$  due to Geometrical Frustration, *Phys. Rev. Lett.* 99 (2007), 256402, <https://doi.org/10.1103/PhysRevLett.99.256402>.
- [13] A.P. Douvalis, V. Papaefthymiou, A. Moukarika, T. Bakas, G. Kallias, Mössbauer and magnetization studies of  $\text{Fe}_2\text{BO}_4$ , *J. Phys.: Condensed Matter* 12 (2000) 177, <https://doi.org/10.1088/0953-8984/12/2/307>.
- [14] P. Bordet, E. Suard, Magnetic structure and charge ordering in  $\text{Fe}_3\text{BO}_5$ : A single-crystal x-ray and neutron powder diffraction study, *Phys. Rev. B* 79 (2009), 144408, <https://doi.org/10.1103/PhysRevB.79.144408>.
- [15] S.R. Bland, M. Angst, S. Adiga, V. Scagnoli, R.D. Johnson, J. Herrero-Martin, P. D. Hatton, Symmetry and charge order in  $\text{Fe}_2\text{OBO}_3$  studied through polarized resonant x-ray diffraction, *Phys. Rev. B* 82 (2010), 115110, <https://doi.org/10.1103/PhysRevB.82.115110>.
- [16] M. Matos, J. Terra, D.E. Ellis, A.S. Pimentel, First principles calculation of magnetic order in a low-temperature phase of the iron ludwigite, *J. Magn. Magn. Mater.* 374 (2015) 148–152, <https://doi.org/10.1016/j.jmmm.2014.08.025>.
- [17] E. Vallejo, M. Avignon, Spin and charge ordering in three-leg ladders in oxyborates, *Phys. Rev. Lett.* 97 (2006), 217203, <https://doi.org/10.1103/PhysRevLett.97.217203>.
- [18] J. Bartolomé, A. Arauzo, N.V. Kazak, N.B. Ivanova, S.G. Ovchinnikov, Y. V. Knyazev, I.S. Lyubutin, Uniaxial magnetic anisotropy in  $\text{Co}_{2.25}\text{Fe}_{0.75}\text{O}_2\text{BO}_3$  compared to  $\text{Co}_3\text{O}_2\text{BO}_3$  and  $\text{Fe}_3\text{O}_2\text{BO}_3$  ludwigites, *Phys. Rev. B* 83 (2011), 144426, <https://doi.org/10.1103/PhysRevB.83.144426>.
- [19] I. Leonov, A.N. Yaresko, V.N. Antonov, J.P. Attfield, V.I. Anisimov, Charge order in  $\text{Fe}_2\text{OBO}_3$ : An LSDA+U study, *Phys. Rev. B* 72 (2005), 014407, <https://doi.org/10.1103/PhysRevB.72.014407>.
- [20] M. Huber, H.J. Deiseroth, Crystal structure of titanium (III) borate,  $\text{TiBO}_3$ , *Zeitschrift für Kristallographie* 210 (1995) 685, <https://doi.org/10.1524/zkri.1995.210.9.685>.
- [21] T.A. Bither, C.G. Frederick, T.E. Gier, J.F. Weiher, H.S. Young, Ferromagnetic  $\text{VBO}_3$  and antiferromagnetic  $\text{CrBO}_3$ , *Solid State Commun.* 8 (1970) 109–112, [https://doi.org/10.1016/0038-1098\(70\)90582-X](https://doi.org/10.1016/0038-1098(70)90582-X).
- [22] X. Zeng, Q. Kuang, Q. Fan, Y. Dong, Y. Zhao, S. Chen, S. Liu, Synthesis, structure, and electrochemical performance of  $\text{V}_3\text{BO}_6$  nanocomposite: A new vanadium borate as high-rate anode for Li-ion batteries, *Electrochimica Acta* 335 (2020), 135661, <https://doi.org/10.1016/j.electacta.2020.135661>.
- [23] N.V. Kazak, M.S. Platunov, Y.V. Knyazev, N.B. Ivanova, O.A. Bayukov, A. D. Vasiliev, S.G. Ovchinnikov, Uniaxial anisotropy and low-temperature

- antiferromagnetism of  $\text{Mn}_2\text{BO}_4$  single crystal, *J. Magn. Magn. Mater.* 393 (2015) 316–324, <https://doi.org/10.1016/j.jmmm.2015.05.081>.
- [24] A. Utzolino, K. Bluhm, New Insights into the Stabilization of the Hulsite Structure During Crystal Structure Determination of  $\text{MnI}_2\text{MnIII}(\text{BO}_3)_2$  and  $\text{MnIIISrMnIII}(\text{BO}_3)_2$ , *Zeitschrift für Naturforschung B* 51 (1996) 1433–1438, <https://doi.org/10.1515/znb-1996-1012>.
- [25] J.C. Fernandes, F.S. Sarrat, R.B. Guimaraes, R.S. Freitas, M.A. Continentino, A.C. Doriguetto, and J. Dumas, Structure and magnetism of  $\text{MnMgB}_2\text{O}_5$  and  $\text{Mn}_2\text{B}_2\text{O}_5$ , *Phys. Rev. B* 67 (2003) 104413, <https://doi.org/10.1103/PhysRevB.67.104413>.
- [26] R.E. Newnham, R.P. Santoro, P.F. Seal, G.R. Stallings, Antiferromagnetism in  $\text{Mn}_3\text{B}_2\text{O}_6$ ,  $\text{Co}_3\text{B}_2\text{O}_6$ , and  $\text{Ni}_3\text{B}_2\text{O}_6$ , *Physica Status Solidi (b)* 16 (1966) K17–K19, <https://doi.org/10.1002/pssb.19660160140>.
- [27] T. Kawano, H. Morito, H. Yamane, Synthesis and characterization of manganese and cobalt pyroborates:  $\text{M}_2\text{B}_2\text{O}_5$  (M = Mn, Co), *Solid state sciences* 12 (2010) 1419–1421, <https://doi.org/10.1016/j.solidstatesciences.2010.05.021>.
- [28] N.B. Ivanova, A.D. Vasil'ev, D.A. Velikanov, N.V. Kazak, S.G. Ovchinnikov, G. A. Petrákovskii, V.V. Rudenko, Magnetic and electrical properties of cobalt oxyborate  $\text{Co}_3\text{BO}_5$ , *Phys. Solid State* 49 (2007) 651–653, <https://doi.org/10.1134/S1063783407040087>.
- [29] J.L.C. Rowsell, L.F. Nazar, Synthesis, structure, and solid-state electrochemical properties of  $\text{Cr}_3\text{BO}_6$ : a new chromium (III) borate with the norbergite structure, *J. Mater. Chem.* 11 (2001) 3228–3233, <https://doi.org/10.1039/B100707F>.
- [30] K. Kudo, T. Noji, Y. Koike, Antiferromagnetic ordering in single-crystal  $\text{Cu}_3\text{B}_2\text{O}_6$ , *J. Phys. Soc. Jpn.* 70 (2001) 935–938, <https://doi.org/10.1143/JPSJ.70.935>.
- [31] E.M. Carnicom, K. Górnicka, T. Klimczuk, R.J. Cava, The homometallic warwickite  $\text{V}_2\text{OBO}_3$ , *J. Solid State Chem.* 265 (2018) 319–325, <https://doi.org/10.1016/j.jssc.2018.06.021>.
- [32] H. Hagiwara, H. Sato, M. Iwaki, Y. Narumi, K. Kindo, Quantum magnetism of perfect spin tetrahedra in  $\text{Co}_4\text{B}_6\text{O}_{13}$ , *Phys. Rev. B* 80 (2009), 014424, <https://doi.org/10.1103/PhysRevB.80.014424>.
- [33] A. Utzolino, K. Bluhm, Synthesis and Crystal Structure of Cobalt Containing Borate Oxides:  $\text{Co}_{1.5}\text{Ti}_{0.5}(\text{BO}_3)_2\text{O}$  and  $\text{Co}_{1.5}\text{Zr}_{0.5}(\text{BO}_3)_2\text{O}$ , *Zeitschrift für Naturforschung B* 50 (1995) 1653–1657, <https://doi.org/10.1515/znb-1995-1111>.
- [34] See Supplemental Material at [URL] for “ $\text{Co}_{5/3}\text{Nb}_{1/3}\text{BO}_4$ : a new cobalt oxyborate with a complex magnetic structure”.
- [35] G.M. Sheldrick, A short history of SHELX, *Acta Cryst. A* 64 (2008) 112–122, <https://doi.org/10.1107/S0108767307043930>.
- [36] G.M. Sheldrick, SHELXS and SHELXL97, Program for Crystal Structure Refinement, University of Göttingen, Germany (1997).
- [37] N.V. Kazak, M.S. Platonov, Y.V. Knyazev, N.B. Ivanova, Y.V. Zubavichus, A. A. Veligzhanin, J. Bartolome, Crystal and local atomic structure of  $\text{MgFeBO}_4$ ,  $\text{Mg}_{0.5}\text{Co}_{0.5}\text{FeBO}_4$  and  $\text{CoFeBO}_4$ : Effects of Co substitution, *Phys. Status Solidi (b)* 252 (2015) 2245–2258, <https://doi.org/10.1002/pssb.201552143>.
- [38] N.E. Brese, M. O'keeffe, Bond-valence parameters for solids, *Acta Cryst. B* 47 (1991) 192–197, <https://doi.org/10.1107/S0108768190011041>.
- [39] J.J. Capponi, J. Chenavas, J.C. Joubert, Sur de nouveaux borates mixtes des métaux de transition isotopes de la warwickite, *J. Solid State Chem.* 7 (1973) 49–54, [https://doi.org/10.1016/0022-4596\(73\)90120-5](https://doi.org/10.1016/0022-4596(73)90120-5).
- [40] R.D. Shannon, Revised effective ionic radii and systematic studies of interatomic distances in halides and chalcogenides, *Acta Crystallogr. Sect. A* 32 (1976) 751, <https://doi.org/10.1107/S0567739476001551>.
- [41] N.V. Kazak, N.A. Belskaya, E.M. Moshkina, L.N. Bezmaternykh, A.D. Vasiliev, S. N. Sofronova, S.G. Ovchinnikov, Antiferromagnetism of the cation-ordered warwickite system  $\text{Mn}_{2-x}\text{Mg}_x\text{BO}_4$  ( $x = 0.5, 0.6$  and  $0.7$ ), *J. Magn. Magn. Mater.* 507 (2020), 166820, <https://doi.org/10.1016/j.jmmm.2020.166820>.
- [42] N.V. Kazak, M.S. Platonov, Y.V. Knyazev, E.M. Moshkina, S.Y. Gavrilkin, O. A. Bayukov, S.G. Ovchinnikov, Fe-induced enhancement of antiferromagnetic spin correlations in  $\text{Mn}_{2-x}\text{Fe}_x\text{BO}_4$ , *J. Magn. Magn. Mater.* 452 (2018) 90–99, <https://doi.org/10.1016/j.jmmm.2017.12.037>.
- [43] A. Arauzo, N.V. Kazak, N.B. Ivanova, M.S. Platonov, Y.V. Knyazev, O.A. Bayukov, J. Bartolomé, Spin-glass behavior in single crystals of hetero-metallic magnetic warwickites  $\text{MgFeBO}_4$ ,  $\text{Mg}_{0.5}\text{Co}_{0.5}\text{FeBO}_4$ , and  $\text{CoFeBO}_4$ , *J. Magn. Magn. Mater.* 392 (2015) 114–125, <https://doi.org/10.1016/j.jmmm.2015.05.006>.
- [44] G. Liang, K. Park, J. Li, Anisotropy in magnetic properties and electronic structure of single-crystal  $\text{LiFePO}_4$ , *Phys. Rev. B* 77 (2008), 064414, <https://doi.org/10.1103/PhysRevB.77.064414>.
- [45] A. Apostolov, M. Mikhov, P. Tcholakov, Magnetic properties of boron ferrites  $\text{FeBMeO}_4$ , *Phys. Status Solidi* 56 (1979) K33–K36.
- [46] N.V. Kazak, M.S. Platonov, Yu.V. Knyazev, M.S. Molokeev, M.V. Gorev, S. G. Ovchinnikov, Z.V. Pchelkina, V.V. Gapontsev, S.V. Streltsov, J. Bartolomé, A. Arauzo, V.V. Yumashev, S.Yu. Gavrilkin, F. Wilhelm, A. Rogalev, Spin state crossover in  $\text{Co}_3\text{BO}_5$ , *Phys. Rev. B* 103 (2021) 094445, <https://doi.org/10.1103/PhysRevB.103.094445>.
- [47] N.V. Kazak, M.S. Platonov, N.B. Ivanova, Yu.V. Knyazev, L.N. Bezmaternykh, E. V. Eremin, A.D. Vasil'ev, Crystal structure and magnetization of a  $\text{Co}_2\text{B}_2\text{O}_6$  single crystal, *JETP* 117 (2013) 94–107, <https://doi.org/10.1134/S1063776113060186>.
- [48] T. Yang, Y. Wang, D. Yang, G. Li, J. Lin, Field-induced spin-flop-like metamagnetism in  $\alpha\text{-CoB}_4\text{O}_7$ , *Solid State Sciences* 19 (2013) 32–35, <https://doi.org/10.1016/j.solidstatesciences.2013.02.014>.
- [49] W. Gou, Zh. He, M. Yang, W. Zhang, W. Cheng, Synthesis and magnetic properties of a new borophosphate  $\text{SrCo}_2\text{BPO}_7$  with a four-column ribbon structure, *Inorg. Chem.* 52 (2013) 2492–2496, <https://doi.org/10.1021/ic3023979>.
- [50] N.B. Ivanova, N.V. Kazak, Y.V. Knyazev, D.A. Velikanov, L.N. Bezmaternykh, S. G. Ovchinnikov, G.S. Patrin, Crystal structure and magnetic anisotropy of ludwigite  $\text{Co}_2\text{FeO}_2\text{B}_3$ , *JETP* 113 (2011) 1015–1024, <https://doi.org/10.1134/S1063776111140172>.